Published June 13, 2016

Local RhoA activation induces cytokinetic furrows independent of spindle position and cell cycle stage

Elizabeth Wagner and Michael Glotzer

Department of Molecular Genetics and Cell Biology, The University of Chicago, Chicago, IL 60637

The GTPase RhoA promotes contractile ring assembly and furrow ingression during cytokinesis. Although many factors that regulate RhoA during cytokinesis have been characterized, the spatiotemporal regulatory logic remains undefined. We have developed an optogenetic probe to gain tight spatial and temporal control of RhoA activity in mammalian cells and demonstrate that cytokinetic furrowing is primarily regulated at the level of RhoA activation. Light-mediated recruitment of a RhoGEF domain to the plasma membrane leads to rapid induction of RhoA activity, leading to assembly of cytokinetic furrows that partially ingress. Furthermore, furrow formation in response to RhoA activation is not temporally or spatially restricted. RhoA activation is sufficient to generate furrows at both the cell equator and cell poles, in both metaphase and anaphase. Remarkably, furrow formation can be initiated in rounded interphase cells, but not adherent cells. These results indicate that RhoA activation is sufficient to induce assembly of functional contractile rings and that cell rounding facilitates furrow formation.

Introduction

In cytokinesis, the final stage of cell division, an actomyosin-based contractile ring physically divides the cell into two genetically equivalent daughter cells. Our understanding of cytokinesis has been greatly influenced by classical experiments in which spindles and/or cells were repositioned or micromanipulated. These perturbations demonstrated that the spindle induces furrow formation during a specific time interval after anaphase onset (Rappaport, 1985). At a molecular level, the small GTPase, RhoA, serves as an essential, dosage-sensitive regulator of cleavage furrow formation in metazoan cells (Kishi et al., 1993; Fededa and Gerlich, 2012; Loria et al., 2012). RhoA serves as a molecular switch that is active when bound to GTP. Once active, RhoA binds to effectors including a diaphanous-related formin to induce F-actin assembly (Otomo et al., 2005; Watanabe et al., 2008) and Rho kinase to activate nonmuscle myosin II (Kosako et al., 2000). Through these and other effectors, RhoA regulates the dynamic changes in actomyosin required for cleavage furrow formation.

RhoA activation during cytokinesis is spatially and temporally regulated and dependent on the RhoGEF Ect2 (Tatsumoto et al., 1999). Ect2 localization and activation are regulated by phospho-dependent interactions with centralspindlin, a protein complex that accumulates on the spindle midzone during anaphase (Yüce et al., 2005; Burkard et al., 2009; Wolfe et al., 2009; Zhang and Glotzer, 2015; Fig. 1 A). This complex also accumulates on the cortex, where it directs local RhoA activation (Basant et al., 2015). Despite extensive research, several questions concerning the regulation of cytokinesis remain unanswered. Is local activation of RhoA sufficient to generate a cleavage furrow, or are other factors required for furrow formation in parallel with RhoA? Are there spatial or temporal requirements for RhoA-mediated contractile ring assembly and furrow formation?

Answers to these fundamental questions require the ability to spatially and temporally manipulate cytokinesis at the molecular level—in particular, at the level of RhoA activation. Optogenetic tools provide precise control of protein localization. In many cases, control of localization allows control of protein activity (Strickland et al., 2012; Toettcher et al., 2013). We engineered an optogenetic tool to manipulate RhoA activity and used it to demonstrate that local activation of RhoA is sufficient to direct cleavage furrow formation.

Results and discussion

Light-mediated control of RhoA activity

Previous iterations of the two-component optogenetic system TULIPs used a membrane-targeted photosensitive domain, LOVpep, in conjunction with a second tag, ePDZ-b1, that binds to LOVpep in a light-dependent manner (Strickland et al., 2012). Here, we substituted the ePDZ-b1 tag with a tandem PDZ tag that is functional in more diverse protein fusions. To manipulate RhoA activation with light, we fused the tandem PDZ tag to the highly specific RhoA guanine nucleotide exchange factor

Correspondence to Michael Glotzer: mglotzer@uchicago.edu

Abbreviations used in this paper: DMD, digital micromirror device; GEF, guanine nucleotide exchange factor; Plk1, polo-like kinase 1.

Supplemental Material can be found at:
http://jcb.rupress.org/content/suppl/2016/06/02/jcb.201603025.DC1.html

The Rockefeller University Press $30.00
J. Cell Biol. Vol. 213 No. 6 641–649
www.jcb.org/cgi/doi/10.1083/jcb.201603025

Published June 13, 2016

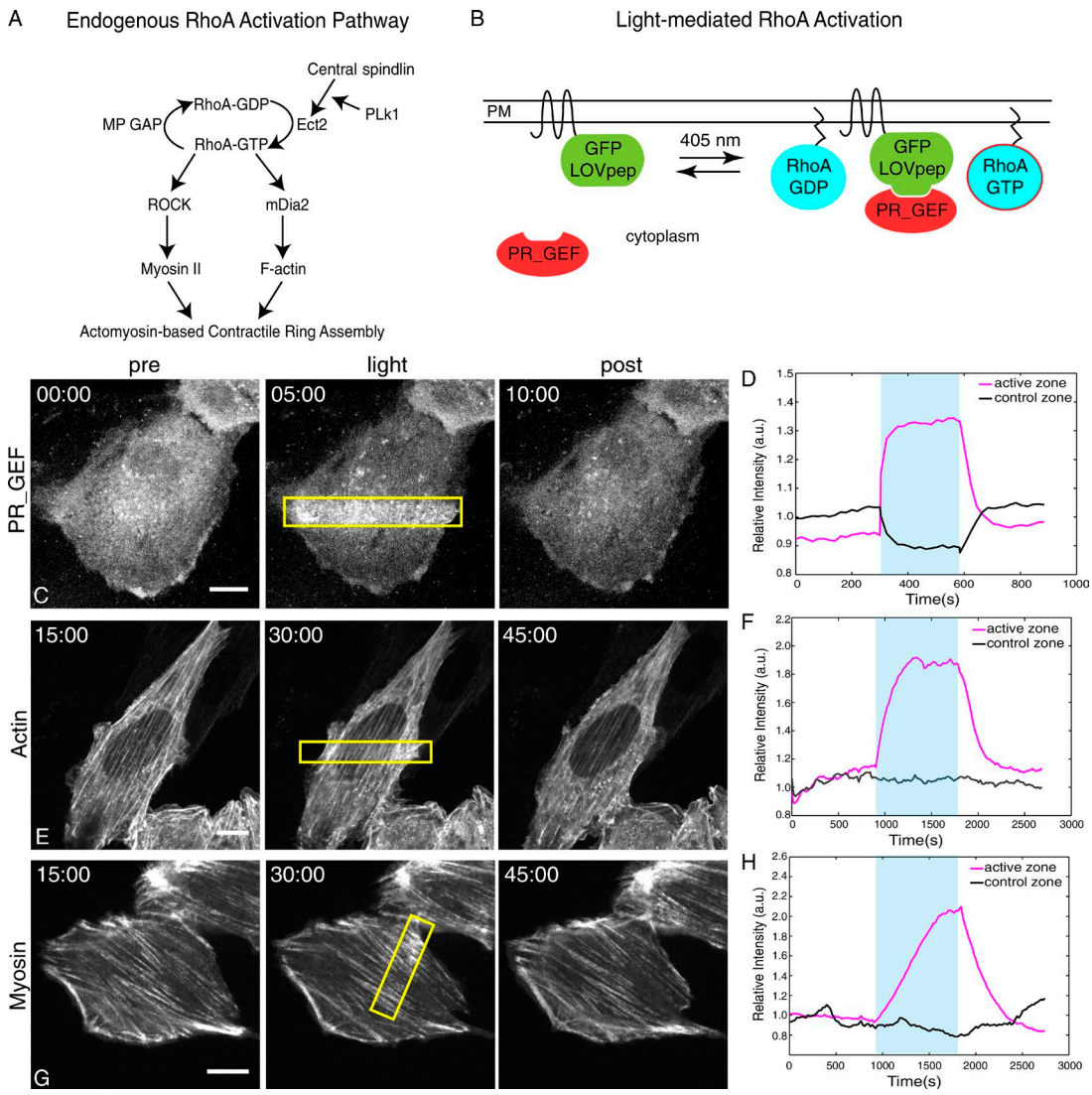

Figure 1. **Light-mediated activation of RhoA.** (A) Schematic depicting the pathway that promotes RhoA activation during cytokinesis. (B) TULIPs-mediated activation of RhoA by light-directed recruitment of PR_GEF. Photoactivation of NIH3T3 cells (yellow boxes) induces local recruitment of PR_GEF (n = 9; C), F-actin polymerization (n = 7; E), and myosin accumulation (n = 15; G). Quantification from representative cells of the relative increase in intensity in the activation region (magenta) vs. a control region (black) for PR_GEF (D), mApple-actin (F), and mCherry-MLC (H) over time. During photoactivation (blue box), cells were locally illuminated (405 nm) with a 960-ms pulse every 20 s. PR_GEF or effectors were imaged every 20 s. a.u., arbitrary units. Bars, 10 µm.

(GEF) LARG (Jaiswal et al., 2011), creating a construct we refer to as photorecruitable GEF (PR_GEF; Fig. 1 B). To reduce basal activity, only the catalytic GEF DH domain was included. GFP-tagged LOVpep was localized to the plasma membrane by fusion to the transmembrane receptor Stargazin. A digital micromirror device (DMD) was used to illuminate arbitrarily defined regions of the cell with 405-nm light. Illumination of adherent cells expressing these constructs resulted in light-mediated local recruitment of PR_GEF (Fig. 1, C and D; and Video 1). Recruitment also led to local accumulation of myosin and F-actin within 20–40 s (Fig. 1, E–H; and Videos 2 and 3). When illumination ceased, the local increase in GEF recruitment was rapidly lost, consistent with the thermal reversion of LOVpep into the dark state (Strickland et al., 2012; $t_{1/2}$ = 80 s; Fig. 1 D). The local increases in actin and myosin were lost with roughly similar kinetics (Fig. 1, F and H), suggesting that RhoA activation is not self-sustaining and implying the existence of RhoGAPs that rapidly inactivate ectopically activated RhoA.

Local activation of RhoA is sufficient to initiate furrow formation at the midzone of anaphase cells

A central question we sought to answer was whether a local zone of RhoA activation is sufficient to form a cleavage furrow. The least stringent test of this model is to determine whether, in a cell progressing normally through anaphase, light-induced RhoA activation can substitute for the endogenous pathway at the equator. Polo-like kinase 1 (Plk1) is required for the phospho-dependent interaction between centralspindlin and Ect2; Plk1 inhibition therefore precludes RhoA activation and furrow formation (Petronczki et al., 2007; Wolfe et al., 2009). This provides an appropriate context for examining whether light-mediated activation of RhoA is sufficient to induce furrow formation.

To generate noncontractile anaphase cells, HeLa cells were arrested in metaphase using a low dose (30 ng/ml) of nocodazole for 4–5 h. Release of the block allowed cells to initiate mitotic exit. Plk1 inhibitor BI 2536 (200 nM) was added 30 min after

Published June 13, 2016

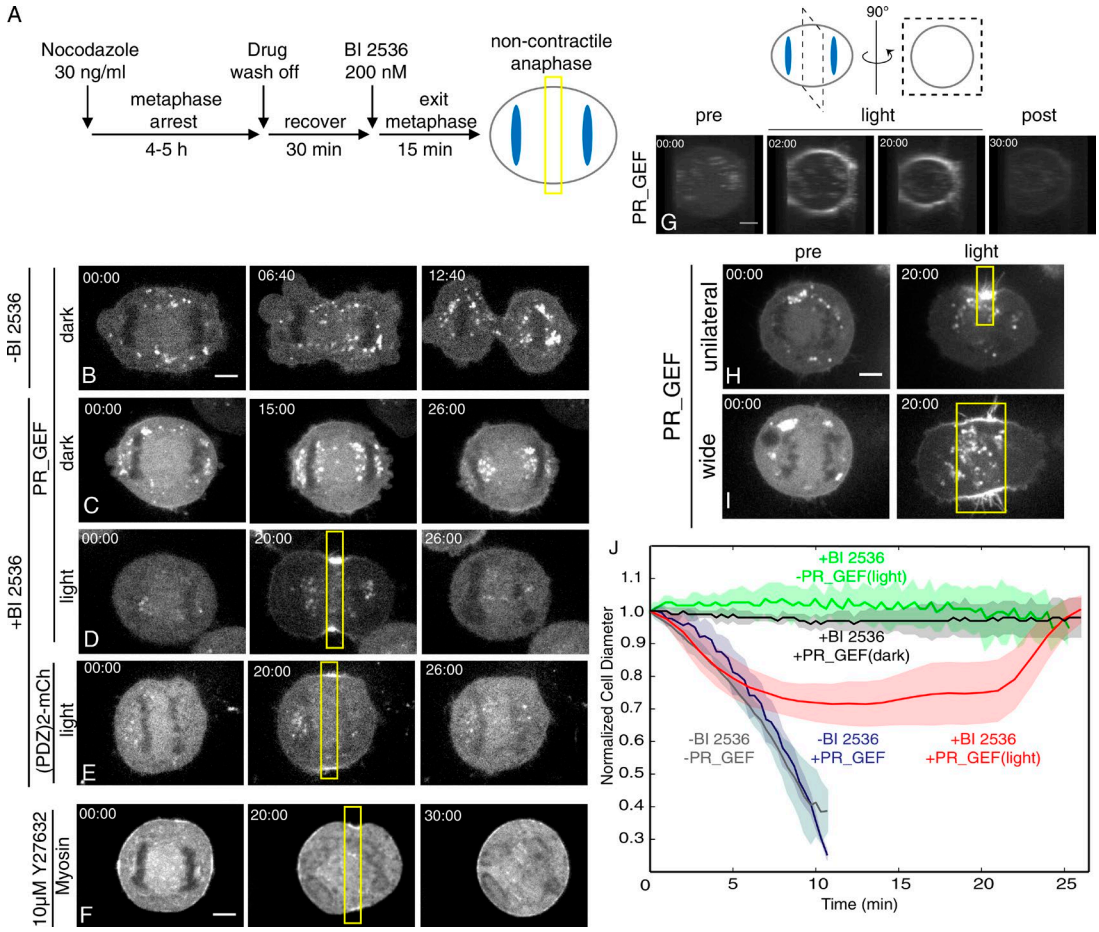

Figure 2. **Local activation of RhoA induces furrow formation in anaphase cells.** (A) Protocol for generating noncontractile anaphase HeLa cells. (B) Images of control HeLa cell expressing PR_GEF dividing normally without illumination (dark). Images of noncontractile anaphase HeLa cells (200 nM BI 2536) expressing PR_GEF (C, D) or PDZ_2-mCh (E) with (yellow boxes; D and E) or without (C) photoactivation. (F) Cell treated as in D in the presence of Rho kinase inhibitor (10 μM Y27632, 30 min). (G) 3D reconstruction of the midzone region of a noncontractile anaphase HeLa cell expressing PR_GEF before (pre), during (light), and after (post) photoactivation. (H and I) Images of cells treated as in D in which the photoactivation zone is restricted (H) or expanded (I). (J) Time course of mean (± SEM) furrow ingression over time of HeLa cells dividing normally (–BI 2536) with (blue, $n = 7$) and without (gray, $n = 10$) PR_GEF expression ($t = 0$ is furrow initiation); noncontractile anaphase cells (+BI 2536) expressing PR_GEF with (red, $n = 32$) and without (black, $n = 6$) local illumination; and locally illuminated noncontractile anaphase cells (+BI 2536) expressing PDZ_2-mCherry (green, $n = 5$; $t = 0$ start of photoactivation or start of imaging for dark controls). For all photoactivation experiments, cells were photoactivated for 20 min followed by 10 min without photoactivation. In all figures, cells are oriented so that the spindle axis is horizontal. a.u., arbitrary units. Bars, 5 μm.

release to block endogenous RhoA activation while permitting anaphase onset (Fig. 2 A; Petronczki et al., 2007). In the absence of PR_GEF recruitment, cells remained noncontractile and furrows did not form (Fig. 2 C). Light-mediated activation of RhoA at the equator was sufficient to initiate formation of a cleavage furrow (Fig. 2 D and Video 4). The initial rate of ingression was similar to that of cells dividing normally in the absence of BI 2536 (Fig. 2 J). This photoactivation protocol zone induced recruitment of PR_GEF to a finely limited region around the entire cell circumference (Fig. 2 G). Notably, light-induced furrows did not fully ingress (~34%, $n = 32$). Furrows resulting from PR_GEF recruitment require the RhoA pathway, as the extent of furrowing was inhibited by Rho kinase inhibitor (5.6 ± 4%; $n = 4$; Fig. 2 F) and recruitment of PDZ_2-mCherry failed to induce furrow formation (Fig. 2 E). In the absence of continued photoactivation, furrows regressed, indicating that RhoA activation during cytokinesis is not self-sustaining under these conditions.

Furrowing activity is restricted to sites of PR_GEF recruitment. Recruitment of PR_GEF to one side of the cell generated a unilateral furrow, and recruitment of PR_GEF to a wide equatorial zone induced equatorial flattening rather than an ingressing furrow (Fig. 2, H and I).

In addition to regulating the Ect2–centralspindlin interaction, Plk1 may promote furrow ingression through other substrates (Neef et al., 2003; Liu et al., 2004; Niiya et al., 2006; Lowery et al., 2007; Wolfe et al., 2009). To generate noncontractile anaphase cells without inhibiting Plk1, cells were depleted of HsCyk4. Light-mediated activation of RhoA in Cyk4-depleted cells induced furrow ingression to 33 ± 5% at 4.2 ± 1.76 μm/min ($n = 6$; Fig. 3, A and B). Thus, light-induced furrowing is similar in Cyk4-depleted and Plk1-inhibited cells, indicating that Plk1 functions primarily upstream of RhoA activation.

To test whether incomplete ingression might be a consequence of the mode of RhoA activation, we induced light-mediated RhoA activation at the equator of cells in which the endogenous pathway for furrow formation was intact. Cells treated in this manner ingressed significantly further than cells induced to furrow by light alone, although they did not fully ingress during 20 min of observation (78.8 ± 9.29% at 3.9 ± 1.56 μm/min, $n = 6$; Fig. 3 C).

Published June 13, 2016

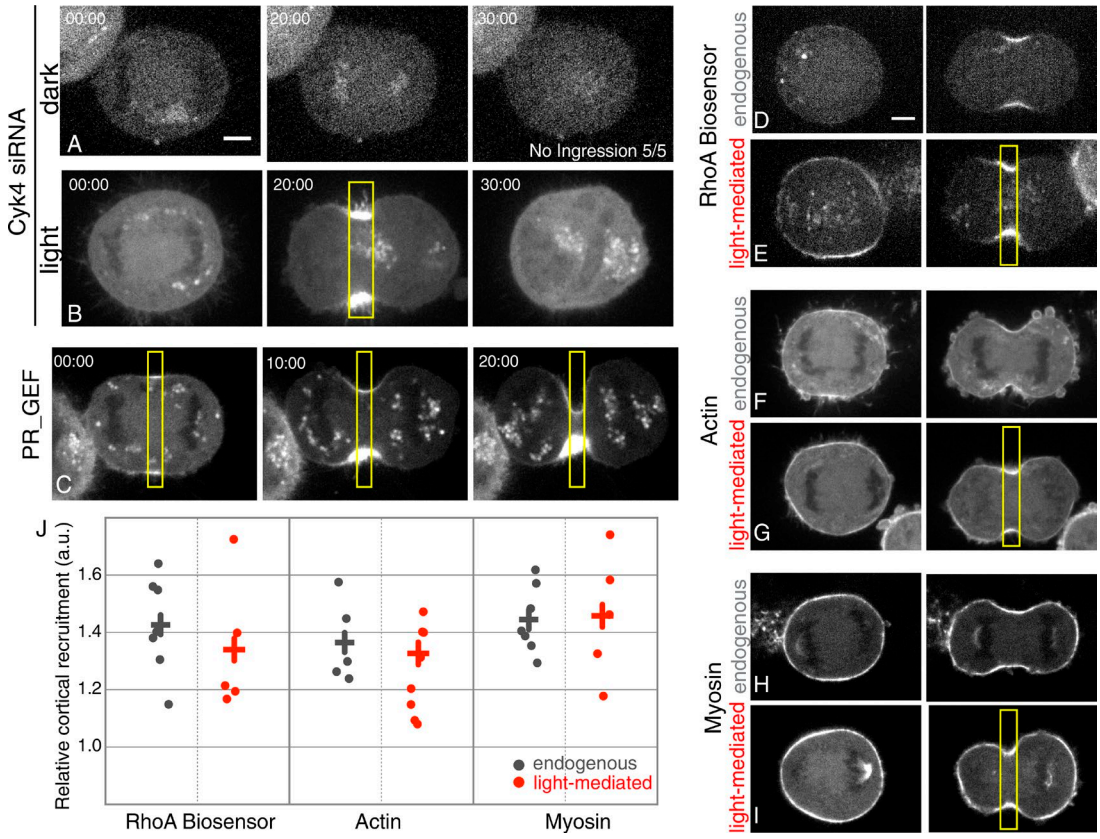

Figure 3. **Characterization of light-induced furrow formation.** Images of anaphase HeLa cells transfected with PR_GEF and Cyk4 siRNA without (A) or with (B) photoactivation. (C) Images of normally dividing HeLa cell expressing PR_GEF just before (t = 0) and during (light) local illumination at the midzone. Comparison of RhoA biosensor (AHDPH-mCherry; D and E), F-actin (mApple-actin; F and G), and myosin (mApple-MLC; H and I) in cells dividing normally and during light-induced furrow formation. (J) Quantification of recruitment of RhoA biosensor, actin, and myosin at endogenous (gray) or light-induced (red) furrows; each dot represents an individual cell and + indicates the mean for that condition. For all photoactivation experiments, cells were locally illuminated for 20 min. Bars, 5 µm.

To examine whether limited ingression was caused by insufficient levels of RhoA activation, we used a RhoA biosensor (Piekny and Glotzer, 2008) to compare the levels of active RhoA in normally dividing cells and cells furrowing in response to PR_GEF recruitment. The distribution and level of active RhoA were comparable (Fig. 3, D, E, and J). In addition, two downstream effectors of RhoA, F-actin and myosin, accumulated at levels comparable to those observed in normally dividing cells (Fig. 3, F–J). Thus, incomplete ingression does not appear to be caused by dramatically reduced activation of RhoA or its key effectors.

The anaphase cortex is uniformly responsive to RhoA activation

We exploited the flexibility that optogenetic tools provide to determine whether the response to RhoA activation is spatially modulated in the anaphase cortex. The anaphase spindle has been shown to play both positive and negative roles in directing RhoA activation and cleavage furrow formation. The central spindle promotes local RhoA activation and cleavage furrow formation at the midzone (Fededa and Gerlich, 2012). Conversely, dynamic astral microtubules play a role in inhibiting cortical contractility in the polar regions (Werner et al., 2007; Zanin et al., 2013; van Oostende Triplet et al., 2014). The spindle may provide positive cues in addition to locally regulating RhoA, such as directed membrane trafficking (Drechsel et al., 1997) and local accumulation of mitotic kinases (Golsteyn et al., 1995; Adams et al., 2001). Thus, induction of active RhoA at cell poles provides a stringent test of whether RhoA activation is sufficient to induce furrowing.

Using the same experimental design in which the endogenous RhoA activation pathway is suppressed by the Plk1 inhibitor, we induced local RhoA activation in a zone spanning the cell poles. RhoA activation was sufficient to initiate furrow formation at this site. These furrows behaved similarly to those at induced at the midzone, ingressing ∼36% at a constriction rate of 4.5 µm/min (Fig. 4, A–C; and Video 5). To directly compare the response to RhoA activation in the midzone versus poles, we simultaneously activated both regions in the same cell. Concurrent illumination of the midzone and poles induced furrows in both regions that ingressed at similar rates and to similar extents (Fig. 4, D–F; and Video 6). To rule out the possibility that excessive PR_GEF recruitment overwhelms the inhibitory effects of astral microtubules, we compared the response at the equator and poles with shorter pulses of light. The duration of the illumination pulse permits tuning of the levels of GEF recruitment and RhoA activation (Fig. S1). We observed simultaneous and similar degrees of furrow induction in the equatorial and polar regions at short activation pulses (Fig. 4 G). We conclude that RhoA activation alone is sufficient to induce cleavage furrow ingression and that the entire cortex is equally responsive to RhoA activation. Furthermore, astral

Published June 13, 2016

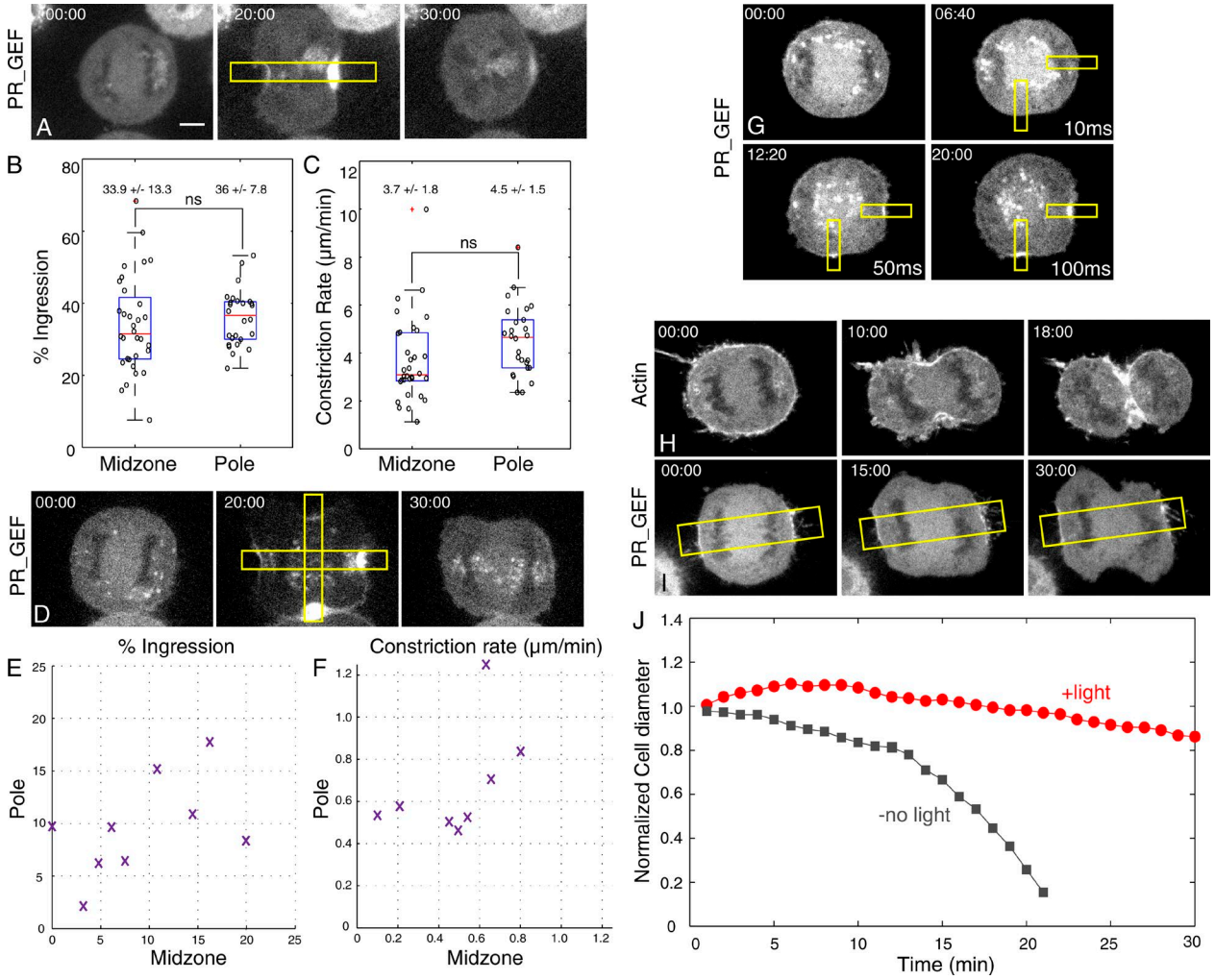

Figure 4. **The anaphase cortex is uniformly responsive to active RhoA.** (A) Images of noncontractile anaphase HeLa cells (200 nm BI 2536) expressing PR_GEF photoactivated (yellow boxes) parallel to the spindle axis. Quantification of the extent of ingression (B) and constriction rate (µm/min; C) of light-induced furrows at cell midzone and poles. (D) Images of noncontractile anaphase HeLa cells (200 nm BI 2536) expressing PR_GEF photoactivated at both the midzone and polar regions. Comparison of the extent of ingression (%; E) and constriction rate (µm/min; F) at the midzone versus pole for individual cells (n = 8). (G) Images of noncontractile anaphase HeLa cells expressing PR_GEF photoactivated with pulses of the indicated duration at the midzone and pole. (H) Images of HeLa cell expressing mApple-Actin undergoing cytokinesis (–BI 2536). (I) Images of HeLa cell expressing PR_GEF undergoing cytokinesis (–BI 2536) with polar photoactivation (n = 5). (J) Ingression kinetics of the endogenous furrow with (red) and without (gray) polar photoactivation in a representative cell. In H and I, cells were photoactivated for 30 min. Bar, 5 µm.

inhibition does not principally act at the level of active GTP-bound RhoA or its downstream effectors, but rather appears to act upstream of RhoA activation.

Because PR_GEF can induce furrowing at the poles, we also assessed the ability of exogenous RhoA activation to compete with the endogenous pathway. Polar recruitment of PR_GEF dramatically slowed ingression of the endogenous furrow, in some cases blocking furrow initiation altogether (Fig. 4, H–J; and Video 7). Although we did not observe deep furrows in the poles in these perturbations, we observed local flattening and suppression of blebbing in the zone of activation, indicating polar activation. This provides additional evidence that the level of RhoA activation induced by PR_GEF is roughly comparable to that of the endogenous furrow.

The response to RhoA activation is not strongly regulated during cell cycle

We next sought to determine whether the response to RhoA activation is temporally regulated. Because the upstream RhoA activation pathway is largely suppressed by Cdk1 activity in metaphase (Yüce et al., 2005), it is not known whether active RhoA or its downstream effectors are subject to cell-cycle regulation. Cells were arrested with 30 ng/ml nocodazole for 4–5 h and released for 20 min to allow assembly of astral microtubules. Before mitotic exit, PR_GEF was locally recruited, resulting in furrow formation. The response to local RhoA activation was similar to that seen during anaphase. Furrows ingressed ∼33% at a rate of ∼4.8 µm/min (Fig. 5, A and B; Fig. S2; and Video 8). Thus, there does not appear to be potent metaphase-specific regulation of active RhoA or its downstream effectors. PR_GEF-induced furrow formation occurred irrespective of whether the zone of illumination was parallel or perpendicular to the metaphase plate, indicating that the response to RhoA activation during metaphase is not spatially regulated.

The consistent response to RhoA activation irrespective of mitotic stage or spindle position prompted us to investigate whether local activation of RhoA can induce furrow formation during interphase. As shown in Fig. 1 (C, E, and G), local activa-

Published June 13, 2016

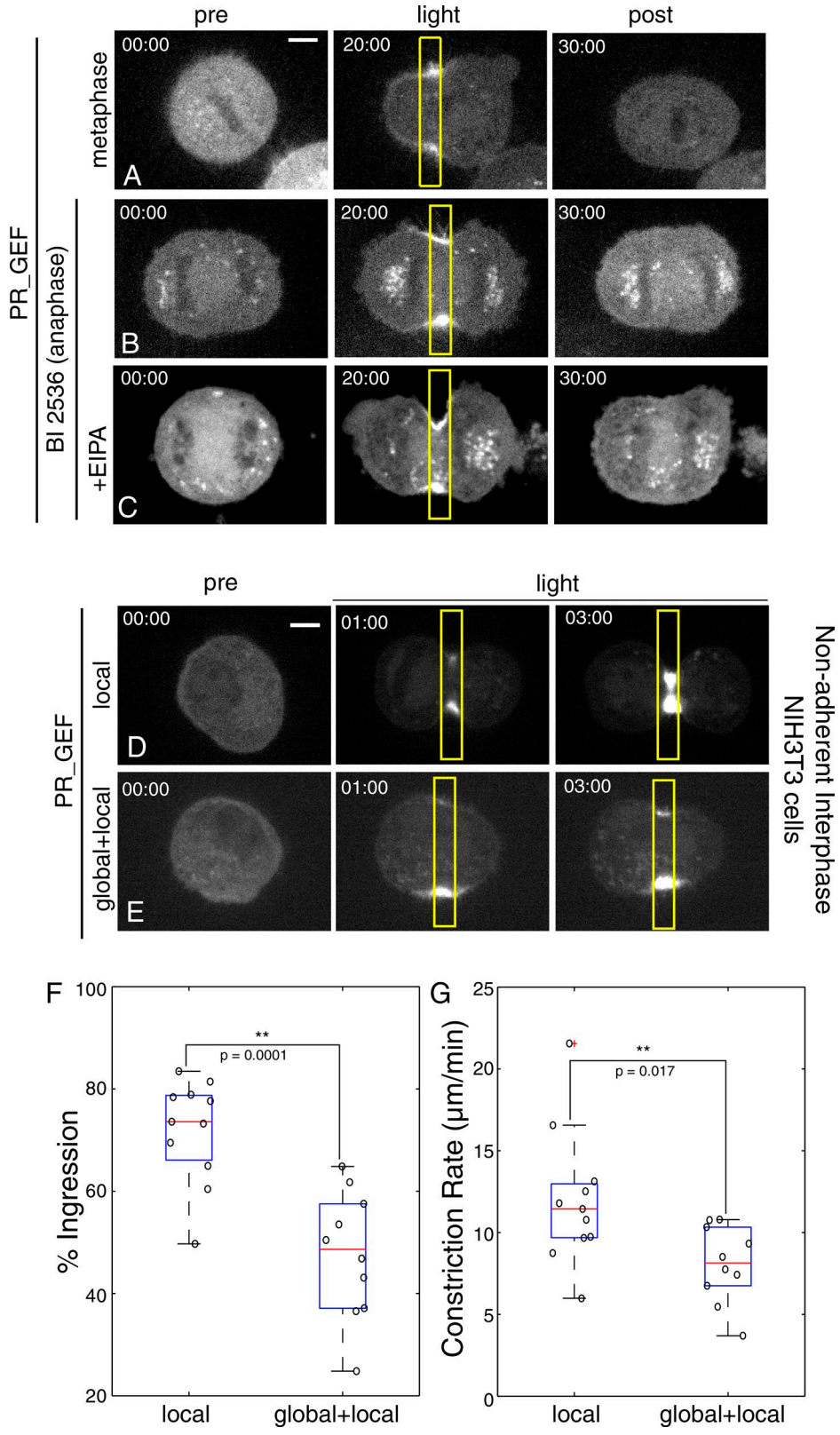

Figure 5. **The response to RhoA activation is not strongly cell-cycle regulated.** Images of photoactivated metaphase HeLa cells (A) and noncontractile (200 nM BI 2536) anaphase HeLa cells without (B) and with (C) 5-(*N*-ethyl-*N*-isopropyl)amiloride (EIPA; 37.5 µM, 30 min). Nonadherent interphase NIH3T3 cells photoactivated only locally (960-ms pulse; D) or supplemented with global illumination (10-ms pulse; E). Quantification of ingression (%; F) and constriction rate (µm/min; G) of nonadherent interphase NIH3T3 cells illuminated as in D and E. Bars, 5 µm.

tion of RhoA in adherent interphase cells promotes F-actin and myosin II accumulation but does not induce furrowing. However, cells entering mitosis remodel their adherence to the substrate and to neighboring cells, allowing them to round (Meyer et al., 2011; Stewart et al., 2011). We hypothesized that a decrease in cell adhesion would alter the response to local RhoA activation in interphase cells. To induce cell detachment and rounding, we treated NIH3T3 cells with trypsin-EDTA before replating. Upon local illumination, cells rapidly formed furrows that ingressed to 72% of completion (Fig. 5 D and Video 9). Similar results were observed in nonadherent interphase HeLa cells (Fig. S3). These results demonstrate that local activation

Published June 13, 2016

of RhoA is sufficient to induce assembly of a contractile ring and that no mitosis-specific factors downstream of RhoA are required for cleavage furrow formation.

Cortical tension modulates furrow ingression in response to local RhoA activation

Exogenous activation of RhoA is sufficient to initiate furrow formation throughout the cell cycle; however, furrows ingress further in nonadherent interphase cells than those in metaphase or anaphase. The distinct mechanical properties of mitotic versus rounded interphase cells may contribute to this differential response. Mitotic entry induces an isotropic increase in cortical tension and hydrostatic pressure concomitant with cell rounding; the rounding pressure is approximately threefold higher in metaphase than in nonadherent interphase cells (Stewart et al., 2011). Enhanced furrow ingression in nonadherent interphase cells could therefore reflect their increased compliance relative to mitotic cells.

We therefore modulated the levels of global cortical tension and assessed whether the response to local RhoA activation was altered in nonadherent interphase cells. In addition to the normal local photoactivation pulse (960 ms), cells were globally illuminated with a short (10-ms) pulse to modestly increase global cortical tension. In comparison to local activation alone, global activation induced a 1.5-fold decrease in both the extent of ingression and the constriction rate (Fig. 5, E–G; and Video 10). Conversely, a global decrease in cortical tension in mitotic cells would be predicted to enhance light-mediated furrow ingression. Upon treatment of noncontractile anaphase cells with the Na/H exchange inhibitor 5-(*N*-ethyl-*N*-isopropyl)amiloride, which has been shown to decrease cortical tension levels of mitotic cells (Stewart et al., 2011), we observed an increase in the extent of furrow ingression (Fig. 5, B and C; 45.6 ± 10% ingression at a rate of 3.84 ± 1.44 µm/min, $n = 8$) compared with untreated cells (33.9 ± 13.3% ingression at a rate of 3.7 ± 1.8 µm/min). These results demonstrate that cortical compliance affects furrow ingression.

RhoA activation is necessary for contractile ring assembly and cleavage furrow formation during cytokinesis (Fededa and Gerlich, 2012). However, whether RhoA activation is the primary control point for cleavage furrow assembly has not been previously examined. An optogenetic approach to control RhoA activation allowed us to molecularly dissect the regulatory logic underlying furrow formation. Exogenous activation of RhoA is sufficient to rescue furrow formation, and the anaphase cortex is uniformly responsive to RhoA activation. These results demonstrate that neither the spindle midzone nor astral microtubules directly regulate active RhoA or its downstream effectors during furrow initiation. Rather, these structures regulate cytokinesis by promoting or inhibiting RhoA activation, respectively.

RhoA activation is also sufficient to induce contractile ring assembly in nonadherent interphase cells. Decreased cell adhesion and rounding are commonly observed in dividing cells (Meyer et al., 2011). Because active RhoA does not induce furrows in adherent cells, our results suggest that furrowing requires both mitotic cell rounding and the ability to generate an equatorial zone of active RhoA.

The response to RhoA activation is not strongly regulated by the cell cycle, as we observed equal furrow formation in metaphase and anaphase cells. The enhanced furrow ingression observed in nonadherent interphase cells may be caused, at least in part, by their reduced cortical tension compared with mitotic cells (Stewart et al., 2011). Thus, we propose that cytokinesis is normally restricted to anaphase because of cell-cycle regulation of cell rounding and the formation of an equatorial zone of active RhoA. We speculate that the central spindle provides a pool of Ect2-centralspindlin that drives complete furrow ingression by activating RhoA with high spatial precision. Accumulating evidence indicates that centralspindlin, Ect2, and RhoA are engaged in a positive feedback loop that may strengthen and sharpen the zone of RhoA activation (Bement et al., 2015; Zhang and Glotzer, 2015), which may contribute to complete furrow ingression during anaphase.

Materials and methods

Cell culture and drug treatment

HeLa and NIH3T3 (ATCC) cells were grown in Dulbecco's modified Eagle's medium (Sigma-Aldrich) supplemented with 10% FBS (Hyclone; Thermo Fisher Scientific), 0.2 mM L-glutamine (Invitrogen), and 1% penicillin/streptomycin (Invitrogen). Where indicated, endogenous HsCyk4 was depleted as described previously (Yüce et al., 2005). For HeLa cell experiments, cells were plated onto glass coverslips 1 d before transfection with plasmid DNA and siRNAs (where applicable) using Lipofectamine 2000 (Invitrogen). For all mitotic cell experiments, 24 h after transfection, HeLa cells were arrested in prometaphase with 30 ng/ml nocodazole (Sigma-Aldrich) for 4–6 h. The nocodazole was washed off, and cells were incubated for 30 min to allow them to recover and exit metaphase. BI-2536 (200 nM; provided by N. Kraut, Boehringer Ingelheim, Berlin, Germany) was then added to block RhoA activation as cells entered anaphase. For NIH3T3 cell experiments, plasmids were transiently transfected using a Neon electroporation system (Invitrogen). For nonadherent HeLa and NIH3T3 cell experiments, cells were trypsinized using 0.05% trypsin-EDTA (Sigma-Aldrich), washed, replated onto glass coverslips, and incubated for 5–10 min to allow minimal adhesion before imaging. HeLa and NIH3T3 cells were differentially suited to the mitotic and interphase experiments: detached interphase HeLa cells are too nonadherent and tend to move during experiments, and NIH3T3 cells are too weakly attached during mitosis for reliable imaging.

Constructs

The optogenetic membrane tether consists of a Stargazin-GFP-LOVpep fusion. Full-length Stargazin (a gift from A. Karginov, University of Illinois at Chicago, Chicago, IL) was used. The LOVpep variant used contains the substitutions T406A, T407A, and I532A (Strickland et al., 2012). The PR_GEF construct consists of a $(PDZ)_2$-mCherry-LARG(DH) fusion protein. The PDZ domain is derived from erbin (Skelton et al., 2003; a gift from S. Koide, The University of Chicago, Chicago IL), which was fused to the DH domain (aa 766–997) of the RhoGEF, LARG (GenBank accession no. NM_015313.2). Flexible linkers ($SAGG_3$ and $SAGG_5$, respectively) were placed between the PDZ domains and between mCherry and the LARG DH domain. PR_GEF^{YFP} was constructed identically, except YFP replaced mCherry. This construct was used in experiments in which the effects on various downstream markers were visualized. To examine the levels of RhoA activation, we used the RhoA biosensor (AHDPH-mCherry; Piekny and Glotzer, 2008). To examine effects on the actin and myosin networks, we used mApple-Actin and mApple-MLC constructs (gifts from M. Davidson, University of Florida, Gainesville, FL).

Live cell imaging and photoactivation

Glass coverslips were placed into an imaging chamber with media supplemented with 10 mM Hepes and 3% Oxyrase (Oxyrase) and main-

Published June 13, 2016

tained at 37°C. Cells were imaged using a 60×, 1.49-NA ApoTIRF oil-immersion objective on a Ti-E inverted microscope (Nikon). The microscope is fitted with a spinning disk confocal (CSU-X1; Yokogawa Electric Corporation) illuminated with a laser merge module containing 491- and 561-nm lasers (Spectral Applied Research). Images were acquired with Coolsnap HQ2 CCD camera (Photometrics). A Mosaic DMD equipped with a 100-mW, 405-nm laser (Photonic Instruments) was used for photoactivation. MetaMorph acquisition software (Molecular Devices) was used to control the microscope hardware. The photoactivation laser was electronically attenuated and optically filtered such that the total incident light if the entire DMD was illuminated at <1 µJ/s. For all photoactivation experiments, unless designated otherwise, the defined region of interest was illuminated for 960 ms every 20 s for 20 min. In some cells, Stargazin-GFP-LOVpep hyperaccumulates in a photoactivation-dependent manner. This hyperaccumulation is not observed upon recruitment of a probe lacking the GEF (2X-PDZ-mCh). Therefore, we infer that cortical contractility can induce concentration of the membrane-tethered probe. When the entire cell was globally activated, an additional 10-ms exposure was added. To select cells for study, confocal images were acquired with 491-nm light followed by 561-nm light, and robust recruitment of PR_GEF was visually confirmed. To examine effects on RhoA activation levels (AHD-mCherry), actin (mApple-actin), or myosin (mApple-MLC), these constructs were coexpressed with Stargazin-GFP-LOVpep and PR_GEF^{YFP}. Cells strongly expressing both the reporter and the membrane tether were chosen for study. In studies in which Stargazin-GFP-LOVpep and PR_GEF were coexpressed, GFP- and mCherry-positive intracellular puncta were observed (Fig. 2), and the number of puncta appeared to increase during photoactivation. We speculate that these are membrane-bound structures that form in response to RhoA activation. These puncta are also present in control experiments using the PDZ_2-mCherry lacking the GEF, albeit at much lower frequencies and without increasing in response to photoactivation.

Image analysis

To quantify the extent and rates of furrow ingression, the position of each side of the ingressing furrow was manually tracked at each time point. The extent of ingression was normalized by measuring the cell diameter between furrow tips and dividing by the initial cell diameter. To measure the accumulation of the RhoA biosensor, actin, and myosin II in furrowing cells, linescans were drawn through the furrow region. For each time point, the maximum intensity, reflecting the cortically localized signal, was measured, as was mean cytoplasmic intensity; recruitment is defined as the ratio of these values. Results shown represent the mean of the maximal recruitment for each cell. In adherent cells, the mean intensity in the activation region was measured and normalized to the initial intensity.

Online supplemental material

Fig. S1 shows that accumulation of PR_GEF and RhoA activation can be tuned by altering the duration of the light pulse. Fig. S2 compares the extent and rate of PR_GEF-induced furrow ingression during anaphase and metaphase. Fig. S3 shows that PR_GEF can induce a deeply ingressing furrow in a rounded HeLa cell. Videos 1–3 show the recruitment of PR_GEF and induction of actin and myosin recruitment in adherent NIH3T3 cells. Videos 4–6 show PR_GEF-mediated induction of furrowing in noncontractile anaphase cells at the equator, poles, and both equator and poles. Video 7 shows the ability of polar recruitment of PR_GEF to inhibit ingression of a endogenous furrow. Video 8 shows PR_GEF-mediated induction of furrowing in a metaphase HeLa cell. Video 9 shows PR_GEF-mediated induction of furrowing in a nonadherent interphase NIH3T3 cell. Video 10 shows that low-level global RhoA activation slows furrowing in a nonadherent interphase NIH3T3 cell. Online supplemental material is available at http://www.jcb.org/cgi/content/full/jcb.201603025/DC1.

Acknowledgments

The authors thank Patrick Oakes and Margaret Gardel for generous access to their imaging system and for sharing routines for quantification and Andrei Karginov, Shohei Koide, and Mike Davidson for generous gifts of plasmids.

This work was supported by National Institute of General Medical Sciences GM085087, and E. Wagner was supported by National Institute of General Medical Sciences T32 GM007183.

The authors declare no competing financial interests.

Submitted: 7 March 2016
Accepted: 18 May 2016

References

Adams, R.R., M. Carmena, and W.C. Earnshaw. 2001. Chromosomal passengers and the (aurora) ABCs of mitosis. *Trends Cell Biol.* 11:49–54. http://dx.doi.org/10.1016/S0962-8924(00)01880-8

Basant, A., S. Lekomtsev, Y.C. Tse, D. Zhang, K.M. Longhini, M. Petronczki, and M. Glotzer. 2015. Aurora B kinase promotes cytokinesis by inducing centralspindlin oligomers that associate with the plasma membrane. *Dev. Cell.* 33:204–215. http://dx.doi.org/10.1016/j.devcel.2015.03.015

Bement, W.M., M. Leda, A.M. Moe, A.M. Kita, M.E. Larson, A.E. Golding, C. Pfeuti, K.-C. Su, A.L. Miller, A.B. Goryachev, and G. von Dassow. 2015. Activator-inhibitor coupling between Rho signalling and actin assembly makes the cell cortex an excitable medium. *Nat. Cell Biol.* 17:1471–1483. http://dx.doi.org/10.1038/ncb3251

Burkard, M.E., J. Maciejowski, V. Rodriguez-Bravo, M. Repka, D.M. Lowery, K.R. Clauser, C. Zhang, K.M. Shokat, S.A. Carr, M.B. Yaffe, and P.V. Jallepalli. 2009. Plk1 self-organization and priming phosphorylation of HsCYK-4 at the spindle midzone regulate the onset of division in human cells. *PLoS Biol.* 7:e1000111. http://dx.doi.org/10.1371/journal.pbio.1000111

Drechsel, D.N., A.A. Hyman, A. Hall, and M. Glotzer. 1997. A requirement for Rho and Cdc42 during cytokinesis in *Xenopus* embryos. *Curr. Biol.* 7:12–23. http://dx.doi.org/10.1016/S0960-9822(06)00023-6

Fededa, J.P., and D.W. Gerlich. 2012. Molecular control of animal cell cytokinesis. *Nat. Cell Biol.* 14:440–447. http://dx.doi.org/10.1038/ncb2482

Golsteyn, R.M., K.E. Mundt, A.M. Fry, and E.A. Nigg. 1995. Cell cycle regulation of the activity and subcellular localization of Plk1, a human protein kinase implicated in mitotic spindle function. *J. Cell Biol.* 129:1617–1628. http://dx.doi.org/10.1083/jcb.129.6.1617

Jaiswal, M., L. Gremer, R. Dvorsky, L.C. Haeusler, I.C. Cirstea, K. Uhlenbrock, and M.R. Ahmadian. 2011. Mechanistic insights into specificity, activity, and regulatory elements of the regulator of G-protein signaling (RGS)-containing Rho-specific guanine nucleotide exchange factors (GEFs) p115, PDZ-RhoGEF (PRG), and leukemia-associated RhoGEF (LARG). *J. Biol. Chem.* 286:18202–18212. http://dx.doi.org/10.1074/jbc.M111.226431

Kishi, K., T. Sasaki, S. Kuroda, T. Itoh, and Y. Takai. 1993. Regulation of cytoplasmic division of *Xenopus* embryo by rho p21 and its inhibitory GDP/GTP exchange protein (rho GDI). *J. Cell Biol.* 120:1187–1195. http://dx.doi.org/10.1083/jcb.120.5.1187

Kosako, H., T. Yoshida, F. Matsumura, T. Ishizaki, S. Narumiya, and M. Inagaki. 2000. Rho-kinase/ROCK is involved in cytokinesis through the phosphorylation of myosin light chain and not ezrin/radixin/moesin proteins at the cleavage furrow. *Oncogene.* 19:6059–6064. http://dx.doi.org/10.1038/sj.onc.1203987

Liu, X., T. Zhou, R. Kuriyama, and R.L. Erikson. 2004. Molecular interactions of Polo-like-kinase 1 with the mitotic kinesin-like protein CHO1/MKLP-1. *J. Cell Sci.* 117:3233–3246. http://dx.doi.org/10.1242/jcs.01173

Loria, A., K.M. Longhini, and M. Glotzer. 2012. The RhoGAP domain of CYK-4 has an essential role in RhoA activation. *Curr. Biol.* 22:213–219. http://dx.doi.org/10.1016/j.cub.2011.12.019

Lowery, D.M., K.R. Clauser, M. Hjerrild, D. Lim, J. Alexander, K. Kishi, S.-E. Ong, S. Gammeltoft, S.A. Carr, and M.B. Yaffe. 2007. Proteomic screen defines the Polo-box domain interactome and identifies Rock2 as a Plk1 substrate. *EMBO J.* 26:2262–2273. http://dx.doi.org/10.1038/sj.emboj.7601683

Meyer, E.J., A. Ikmi, and M.C. Gibson. 2011. Interkinetic nuclear migration is a broadly conserved feature of cell division in pseudostratified epithelia. *Curr. Biol.* 21:485–491. http://dx.doi.org/10.1016/j.cub.2011.02.002

Neef, R., C. Preisinger, J. Sutcliffe, R. Kopajtich, E.A. Nigg, T.U. Mayer, and F.A. Barr. 2003. Phosphorylation of mitotic kinesin-like protein 2 by polo-like kinase 1 is required for cytokinesis. *J. Cell Biol.* 162:863–875. http://dx.doi.org/10.1083/jcb.200306009

Niiya, F., T. Tatsumoto, K.S. Lee, and T. Miki. 2006. Phosphorylation of the cytokinesis regulator ECT2 at G2/M phase stimulates association of the mitotic kinase Plk1 and accumulation of GTP-bound RhoA. *Oncogene.* 25:827–837. http://dx.doi.org/10.1038/sj.onc.1209124

Otomo, T., C. Otomo, D.R. Tomchick, M. Machius, and M.K. Rosen. 2005. Structural basis of Rho GTPase-mediated activation of the formin mDia1. *Mol. Cell.* 18:273–281. http://dx.doi.org/10.1016/j.molcel.2005.04.002

Petronczki, M., M. Glotzer, N. Kraut, and J.-M. Peters. 2007. Polo-like kinase 1 triggers the initiation of cytokinesis in human cells by promoting recruitment of the RhoGEF Ect2 to the central spindle. *Dev. Cell.* 12:713–725. http://dx.doi.org/10.1016/j.devcel.2007.03.013

Piekny, A.J., and M. Glotzer. 2008. Anillin is a scaffold protein that links RhoA, actin, and myosin during cytokinesis. *Curr. Biol.* 18:30–36. http://dx.doi.org/10.1016/j.cub.2007.11.068

Rappaport, R. 1985. Repeated furrow formation from a single mitotic apparatus in cylindrical sand dollar eggs. *J. Exp. Zool.* 234:167–171. http://dx.doi.org/10.1002/jez.1402340120

Skelton, N.J., M.F.T. Koehler, K. Zobel, W.L. Wong, S. Yeh, M.T. Pisabarro, J.P. Yin, L.A. Lasky, and S.S. Sidhu. 2003. Origins of PDZ domain ligand specificity. Structure determination and mutagenesis of the Erbin PDZ domain. *J. Biol. Chem.* 278:7645–7654. http://dx.doi.org/10.1074/jbc.M209751200

Stewart, M.P., J. Helenius, Y. Toyoda, S.P. Ramanathan, D.J. Muller, and A.A. Hyman. 2011. Hydrostatic pressure and the actomyosin cortex drive mitotic cell rounding. *Nature.* 469:226–230. http://dx.doi.org/10.1038/nature09642

Strickland, D., Y. Lin, E. Wagner, C.M. Hope, J. Zayner, C. Antoniou, T.R. Sosnick, E.L. Weiss, and M. Glotzer. 2012. TULIPs: Tunable, light-controlled interacting protein tags for cell biology. *Nat. Methods.* 9:379–384. http://dx.doi.org/10.1038/nmeth.1904

Tatsumoto, T., X. Xie, R. Blumenthal, I. Okamoto, and T. Miki. 1999. Human ECT2 is an exchange factor for Rho GTPases, phosphorylated in G2/M phases, and involved in cytokinesis. *J. Cell Biol.* 147:921–928. http://dx.doi.org/10.1083/jcb.147.5.921

Toettcher, J.E., O.D. Weiner, and W.A. Lim. 2013. Using optogenetics to interrogate the dynamic control of signal transmission by the Ras/Erk module. *Cell.* 155:1422–1434. http://dx.doi.org/10.1016/j.cell.2013.11.004

van Oostende Triplet, C., M. Jaramillo Garcia, H. Haji Bik, D. Beaudet, and A. Piekny. 2014. Anillin interacts with microtubules and is part of the astral pathway that defines cortical domains. *J. Cell Sci.* 127:3699–3710. http://dx.doi.org/10.1242/jcs.147504

Watanabe, S., Y. Ando, S. Yasuda, H. Hosoya, N. Watanabe, T. Ishizaki, and S. Narumiya. 2008. mDia2 induces the actin scaffold for the contractile ring and stabilizes its position during cytokinesis in NIH 3T3 cells. *Mol. Biol. Cell.* 19:2328–2338. http://dx.doi.org/10.1091/mbc.E07-10-1086

Werner, M., E. Munro, and M. Glotzer. 2007. Astral signals spatially bias cortical myosin recruitment to break symmetry and promote cytokinesis. *Curr. Biol.* 17:1286–1297. http://dx.doi.org/10.1016/j.cub.2007.06.070

Wolfe, B.A., T. Takaki, M. Petronczki, and M. Glotzer. 2009. Polo-like kinase 1 directs assembly of the HsCyk-4 RhoGAP/Ect2 RhoGEF complex to initiate cleavage furrow formation. *PLoS Biol.* 7:e1000110. http://dx.doi.org/10.1371/journal.pbio.1000110

Yüce, O., A. Piekny, and M. Glotzer. 2005. An ECT2-centralspindlin complex regulates the localization and function of RhoA. *J. Cell Biol.* 170:571–582. http://dx.doi.org/10.1083/jcb.200501097

Zanin, E., A. Desai, I. Poser, Y. Toyoda, C. Andree, C. Moebius, M. Bickle, B. Conradt, A. Piekny, and K. Oegema. 2013. A conserved RhoGAP limits M phase contractility and coordinates with microtubule asters to confine RhoA during cytokinesis. *Dev. Cell.* 26:496–510. http://dx.doi.org/10.1016/j.devcel.2013.08.005

Zhang, D., and M. Glotzer. 2015. The RhoGAP activity of CYK-4/MgcRacGAP functions non-canonically by promoting RhoA activation during cytokinesis. *eLife*. 4:e08898. http://dx.doi.org/10.7554/eLife.08898